Metastable Materials

DOI: 10.1002/anie.201300644

Orthorhombic In_2O_3: A Metastable Polymorph of Indium Sesquioxide**

*Maged F. Bekheet, Marcus R. Schwarz, Stefan Lauterbach, Hans-Joachim Kleebe, Peter Kroll, Ralf Riedel, and Aleksander Gurlo**

Indium oxide (In_2O_3), a transparent semiconductor with intrinsic n-type character, serves as a base material for diverse applications, including touch displays and photovoltaics,[1] thermoelectrics,[2] and gas sensors.[3] The synthesis of macroscopic quantities of indium oxide polymorphs as well as growth of their single crystals is of great interest for technology and fundamental science because their physicochemical characterization will significantly enhance the structure–property understanding in indium oxide.[4] For instance, the control of the electronic structure in In_2O_3 polymorphs is required for guiding synthetic approaches towards transparent conductive oxides with improved optical and electronic properties.[5] Four In_2O_3 polymorphs have been synthesized to date, namely: 1) cubic bixbyite-type c-In_2O_3 (C-type structure of rare-earth oxides, $Ia\bar{3}$, No. 206); 2) rhombohedral corundum-type rh-In_2O_3 (space group $R\bar{3}c$, No. 167); 3) orthorhombic Rh_2O_3(II)-type o′-In_2O_3 (*Pbcn*, No. 60); and 4) orthorhombic α-Gd_2S_3-type o″-In_2O_3 (*Pnma*, No. 62). c-In_2O_3 and rh-In_2O_3 are accessible through solution-based and solvothermal routes;[6] α-Gd_2S_3-type o″-In_2O_3 is attainable at pressures over 19.9 GPa, and it transforms to rh-In_2O_3 upon decompression.[7] The synthesis and stability of the first orthorhombic polymorph (o′-In_2O_3) faces some controversy. According to the literature,[8] o′-In_2O_3 is stable in the pressure range between 8.1 and 19.9 GPa, but ultimately transforms to rh-In_2O_3 upon decompression. In contrast, we succeeded in the recovery from circa 30 GPa to ambient pressure and temperature in a laser-heated diamond anvil cell experiment.[9] However, owing to a very limited amount of the specimen (a few crystals, $< 10^{-4}$ mm^3) the crystal structure of o′-In_2O_3 under ambient conditions was not unambiguously confirmed. As our results led to some discussion in the community,[10] we set out to explore alternative high-pressure routes towards a large amount of the o′-In_2O_3 polymorph. The main goals of this work are as follows: 1) to synthesize macroscopic quantities of o′-In_2O_3; 2) to recover it to ambient pressure; and 3) to determine the crystal structure of o′-In_2O_3 under ambient conditions. It is important to note that other corundum-type sesquioxides, including Cr_2O_3,[11] Fe_2O_3,[12] and Al_2O_3,[13] transform to Rh_2O_3(II)-type structure under high pressure, but none of them have been recovered to ambient conditions to date. Therefore, the availability of Rh_2O_3(II)-type o′-In_2O_3 under ambient conditions will also contribute to better understanding of the structural chemistry and properties of other binary oxides.

Our work differs from the previous studies[7,9,14] in three major aspects. First, we are guided by theoretical calculations that suggest using the metastable corundum-type rh-In_2O_3 (for the specimen details we refer to references [6,15]) as starting material for the high-pressure synthesis of the orthorhombic o′-In_2O_3 polymorph. Computations indicate that o′-In_2O_3 is lower in enthalpy than the rh-In_2O_3 for pressures above 6.4 GPa (arrow 1 in Figure 1a) and thus below the c- to o′-In_2O_3 transition (arrow 2 in Figure 1a).[6]

Both structures, rh-In_2O_3 and o′-In_2O_3, are connected by a diffusionless pathway via a common monoclininc *P*2/*c* subgroup (in analogy to Al_2O_3).[10a] We computed the activation barrier for the collective transition rh-In_2O_3→o′-In_2O_3 to 0.08 eV per atom, which corresponds to a temperature of about 650 °C at the transition pressure (Figure 1b). Consequently, we expect a fast transformation rh-In_2O_3→o′-In_2O_3 under high-pressure high-temperature conditions.

Second, as we aim at high-yield synthesis, we choose multi-anvil and toroid cell apparatus that allowed us to obtain macroscopic quantities (ca. 10–100 mm^3) of o′-In_2O_3 polymorphs and also to grow macroscopic single crystals.[16] The synthesis in multi-anvil cells is considered as a step towards an industrial scale synthesis, for example, in a belt apparatus that allows circa 7 cm^3 of material to be obtained under given conditions; a similar pressure is applied in industrial synthesis of diamond and cubic boron nitride.[17] Finally, we perform time-resolved synchrotron studies in multi-anvil assemblies to

[*] M. F. Bekheet, Dr. S. Lauterbach, Prof. Dr. H.-J. Kleebe, Prof. Dr. R. Riedel, Priv.-Doz. Dr. A. Gurlo
Fachbereich Material- und Geowissenschaften
Technische Universität Darmstadt
64287 Darmstadt (Germany)
E-mail: gurlo@materials.tu-darmstadt.de
Dr. M. R. Schwarz
Technische Universität-Bergakademie Freiberg, Freiberg High Pressure Research Centre, Institut für Anorganische Chemie
09599 Freiberg (Germany)
Prof. Dr. P. Kroll
Department of Chemistry and Biochemistry
The University of Texas at Arlington
Arlington, TX 760019-0065 (USA)

[**] Financial support by the German Research Foundation within the priority programme SPP1236 and DESY are greatly acknowledged. The authors thank Christian Lathe for technical support and the Helmholtz Centre Potsdam, GFZ German Research Centre for Geosciences, for the opportunity to perform experiments at the MAX200X press.

Supporting information for this article is available on the WWW under http://dx.doi.org/10.1002/anie.201300644. Further details of the crystal structure investigations may be obtained from the Fachinformationszentrum Karlsruhe, 76344 Eggenstein-Leopoldshafen, Germany (fax: (+49) 7247-808-666; e-mail: crysdata@fiz-karlsruhe.de), on quoting the depository number CSD-425865.

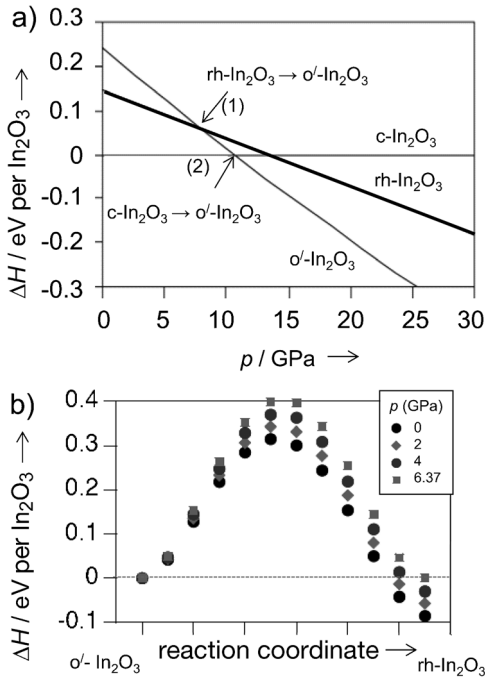

Figure 1. a) A section of the enthalpy–pressure (ΔH–p) diagram for indium oxide polymorphs; c-In_2O_3 is a reference structure. Arrows indicate transitions (1) rh-In_2O_3→o′-In_2O_3 and (2) c-In_2O_3→o′-In_2O_3. b) The relative enthalpy (per formula unit of In_2O_3) between o′-In_2O_3 and rh-In_2O_3 polymorphs at 0, 2, 4, and 6.4 GPa.

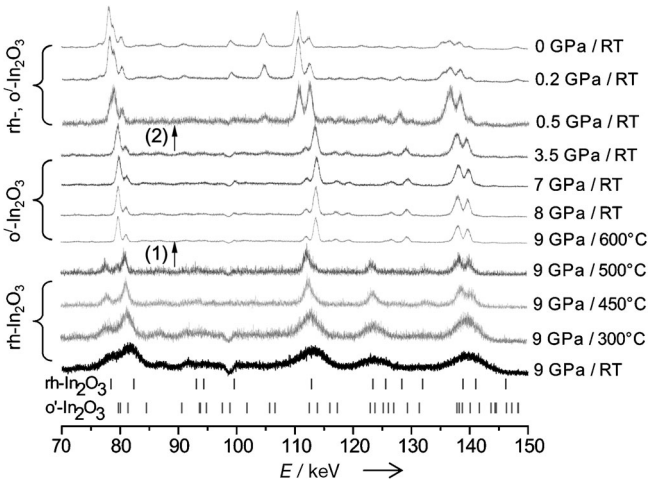

Figure 2. In situ energy-dispersive XRD patterns in multi-anvil assemblies of a rh-In_2O_3 specimen compressed at 9.0 GPa and heated up to 600 °C. The tick marks refer to the calculated Bragg positions of o′-In_2O_3 (bottom) and rh-In_2O_3 (top). Arrows indicate the complete phase transition rh-In_2O_3→o′-In_2O_3 (1) and the partial o′-In_2O_3 transformation to rh-In_2O_3 (2).

follow phase transformations in situ under high-pressure high-temperature conditions. The phase development in rh-In_2O_3 was monitored in situ by energy-dispersive X-ray diffractometry at the two-stage 6–8 MAX200X multi-anvil high-pressure diffractometer of the GFZ Potsdam (beamline W2, HASYLAB/DESY, Hamburg, Germany). New high-pressure/high-temperature multi-anvil assemblies for synchrotron studies developed at the Freiberg High Pressure Research Centre are employed.[18] These assemblies have low X-ray absorption and do not show any additional reflections from the sample environment (see the Supporting Information).[19]

Figure 2 shows the in situ energy-dispersive X-ray diffraction patterns of the rh-In_2O_3 specimen compressed to 9.0 GPa and heated up to 600 °C. XRD patterns observed between ambient pressure and 9.0 GPa at room temperature correspond to rh-In_2O_3 (see also Figure 3 a and Table 1). During compression at room temperature, deviatoric stress causes a significant broadening of XRD reflections. Peak positions are shifted to higher energy (lower d-spacings), indicating a decrease in the volume of the elementary cell. These results are consistent with the previous studies.[8,9] When the sample is heated under constant pressure of 9 GPa, the XRD peaks become narrower because of the release of the internal stress. At 600 °C, the peak intensity of rh-In_2O_3 is significantly reduced and a series of new reflections appears. These reflections represent a characteristic pattern of the orthorhombic o′-In_2O_3 polymorph.

The complete transformation from rh-In_2O_3 to o′-In_2O_3 takes less than 20 seconds at 600 °C and 9 GPa (arrow 1 in Figure 2), indicating fast kinetics as expected for a diffusionless transition. The XRD pattern of material rapidly quenched at 9 GPa from 600 °C to room temperature possesses only o′-In_2O_3 reflections. During decompression at room temperature, o′-In_2O_3 partially transforms to corundum-type rh-In_2O_3 at pressures below 1.0 GPa (arrow 2 in Figure 2).

Table 1: Phase composition of initial and recovered materials.[a]

Specimen	rh-In_2O_3 ($R\bar{3}c$, Z=6)	o′-In_2O_3 ($Pbcn$, Z=4)	o-InOOH ($P2_1nm$, Z=2)
starting material (Figure 3 a)	100 %, a = 5.4814 (5) c = 14.4998(3)	–	–
recovered from 9 GPa/ 600 °C (Figure 3 b)	15.9 % a = 5.4795(4) c = 14.4224	80 % a = 7.9295(1) b = 5.4821(2) c = 5.5898(6)	4.1 % a = 5.2587(9) b = 4.5660(5) c = 3.2669(6)
recovered from 8 GPa/ ca. 1100 °C (Figure 3 c)	31.5 % a = 5.4803(5) c = 14.4484(1)	63.8 % a = 7.9208(1) b = 5.4881(6) c = 5.5977(1)	4.7 % a = 5.2611(8) b = 4.5673(3) c = 3.2709(4)

[a] Fraction (wt %) and lattice parameters a, b, c [Å].

The structure refinement of the specimen recovered to ambient pressure confirms the coexistence of o′-In_2O_3 (fraction: 80.0 wt %), rh-In_2O_3 (15.9 wt %), and o-InOOH (4.1 wt %) as a side phase (Figure 3 b, Table 1).

In the next step, we explored whether the synthesis of o′-In_2O_3 could be reproduced ex situ in a toroid-type high-pressure device that allows even larger macroscopic quantities to be obtained, as well as a fast compression/decompression rate and less experimental preparation times compared to multi-anvil devices.[20] In a typical experiment, rh-In_2O_3 was compressed to 8 GPa and heated at about 1000–

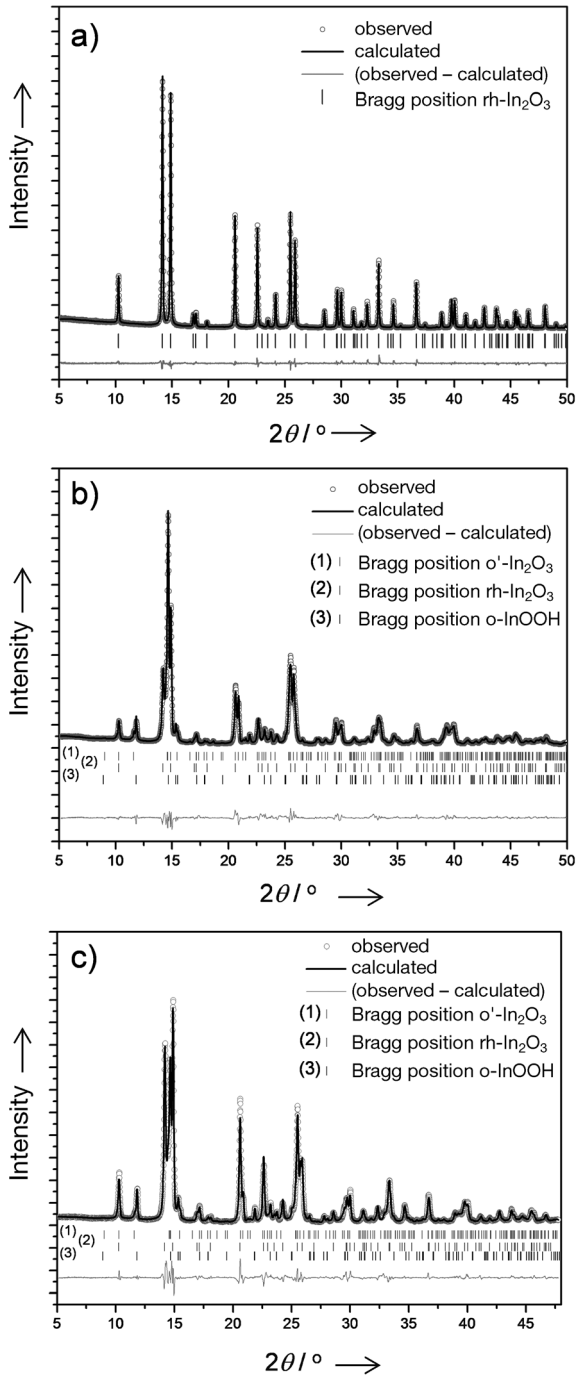

Figure 3. Structure refinement of the starting material rh-In_2O_3 (a) and specimens recovered from the in situ multi-anvil cell (b) and toroid (c) experiments, showing observed and calculated intensities. Tick marks refer to Bragg reflections of o′-In_2O_3, rh-In_2O_3, and o-InOOH (bottom). Table 1 summarizes the results of the structure refinement.

1100 °C for 10 minutes. Figure 3c shows the X-ray powder diffraction pattern and Rietveld difference plot of the recovered specimen. The structure refinement (Figure 3c, Table 1) confirmed our finding from the in situ multi-anvil experiments and shows the coexistence of o′-In_2O_3 (fraction: 63.8 wt%), rh-In_2O_3 (31.5 wt%), and o-InOOH (4.7 wt%). The o-InOOH probably arises from the reaction between In_2O_3 and water under high-pressure and high-temperature (hydrothermal) conditions.[21] Possible water sources include the pressure standard or the sample itself. Interestingly, o-InOOH was also obtained as a side phase in recent synthesis of $InMnO_3$ and In-Mn-Fe-O perovskites and corundum-type $In_{2-2x}Zn_xSn_xO_3$ oxides performed at 6 GPa/1100–1500 °C and 7 GPa/1000 °C, respectively.[22]

Figure 4a displays the high-resolution transmission electron micrograph of a small area (ca. 300 nm^2) of an individual o′-In_2O_3 crystal. Figure 4b shows the diffraction pattern

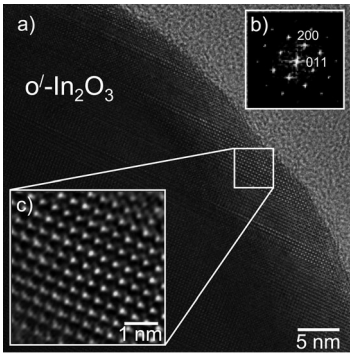

Figure 4. a) High-resolution transmission electron micrograph of a small area (ca. 300 nm^2) of an individual o′-In_2O_3 crystal. b) The diffraction pattern obtained from the boxed area by means of Fourier-filtered transform (FFT) with 200 and 011 spots of the orthorhombic structure. c) Fourier-filtered image from the boxed area. The d-spacings related to the 200 and 011 reflections (3.96 Å and 3.92 Å, respectively) are well-resolved.

obtained from the boxed area by means of Fourier-filtered transform (FFT) with 200 and 011 spots of the orthorhombic structure. Figure 4c is a Fourier-filtered image from the boxed area. The d spacings related to the 200 and 011 reflections (3.96 Å and 3.92 Å, respectively) shown in the inset with the diffraction pattern are well-resolved in the Fourier-filtered image, confirming unambiguously the o′-In_2O_3 structure (*Pbcn*, No. 60, $a = 7.9295(1)$, $b = 5.4821(2)$, $c = 5.5898(6)$ Å).

As the crystal structure data for o′-In_2O_3 at ambient pressure (0 GPa) are in perfect agreement with those reported in theoretical computations[9,23] (Table 2), we demonstrate unambiguously that orthorhombic Rh_2O_3(II)-type o′-In_2O_3 can be recovered to ambient conditions and we provide the first experimental solution of its crystal structure at ambient pressure.

The scanning electron micrographs (Figure 5) visualize the amount of the specimen recovered from the in situ multi-anvil and toroid cell experiments. Figure 5a shows a cross-section of the amorphous SiBCN crucible with the recovered In_2O_3-sample; Figure 5b shows the In_2O_3 specimen in a molybdenum capsule recovered from the toroid cell experiment. The morphology of the o′-In_2O_3 crystals is shown in Figure 5b and c. An apparent porosity in Figure 5c may indicate water evaporation from the cell, which in turn may correspond with formation of o-InOOH as a side phase.

In three In_2O_3 polymorphs, which are available at ambient conditions, indium is octahedrally coordinated and oxygen

Table 2: Crystal structure data of o′-In_2O_3 (*Pbcn*, Nr 60, $Z=4$) at 0 GPa.

Parameter		Theory			Experiment	
		DFT-GGA[a]	IPP[b]	LH-DAC[c]	Multi-anvil[d]	Toroid[d]
a [Å]		8.072	7.96	7.96(3)	7.9295(1)	7.9208(1)
b [Å]		5.588	5.48	5.62(3)	5.4821(2)	5.4881(6)
c [Å]		5.678	5.59	5.52(3)	5.5898(6)	5.5977(1)
In(8d)	*x*	0.1145	–	–	0.11483	0.11534
	y	0.7521			0.74607	0.73407
	z	0.0281			0.02627	0.02359
O1(8d)	*x*	0.8943	–	–	0.85114	0.78409
	y	0.6098			0.61188	0.62484
	z	0.1043			0.09552	0.02174
O2(4c)	*x*	0	–	–	0	0
	y	0.0418			0.03792	0.05453
	z	0.25			0.25	0.25

[a] Density functional theory, generalized gradient approximation.[9] [b] Interatomic pair potential.[23] [c] Laser-heated diamond anvil cell.[9] [d] This work.

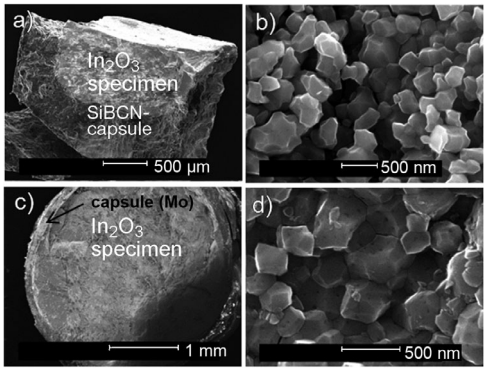

Figure 5. a) Scanning electron micrographs of the specimens recovered from the in situ multi-anvil (a,b) and toroid cell (c,d) experiments. b,d) High-magnification images of o′-In_2O_3 crystals.

tetrahedrally coordinated (Figure 6); the structural differences between them lie in the stacking of {InO_6} octahedra. In c-In_2O_3, the {InO_6} octahedra share corners and edges; in the other two it is the edges and faces. The o′-In_2O_3 is an orthorhombic distortion of the rh-In_2O_3 structure, in which each {InO_6} octahedron shares only two edges with other octahedra rather than three in rh-In_2O_3. The interatomic distances are similar in all three structures; that is, the mean In–O distance is in the range 2.182–2.189 Å. o′-In_2O_3 is the densest polymorph, and the volume reduction from c-In_2O_3 and rh-In_2O_3 to o′-In_2O_3 is about 6 and 3%, respectively.

As both rh-In_2O_3 and o′-In_2O_3 structures are connected by a diffusionless pathway described using the common monoclinic *P*2/*c* subgroup, the transition rh-In_2O_3→o′-In_2O_3 is fast and displacive. In this transition, some oxygen atoms move along the *c* axis (in the *z* direction). In analogy to the corundum-to-Rh_2O_3(II) transition of Al_2O_3,[10a] the majority of In–O bonds is preserved during the rh-In_2O_3→o′-In_2O_3 transition: only one out of 12 In–O bonds per formula unit of In_2O_3 breaks and reforms. The energy required for the aforementioned transformation path is estimated to be about 0.275 eV per formula unit of In_2O_3 (taking a typical In–O bond energy in gaseous InO species).[24] Our calculations

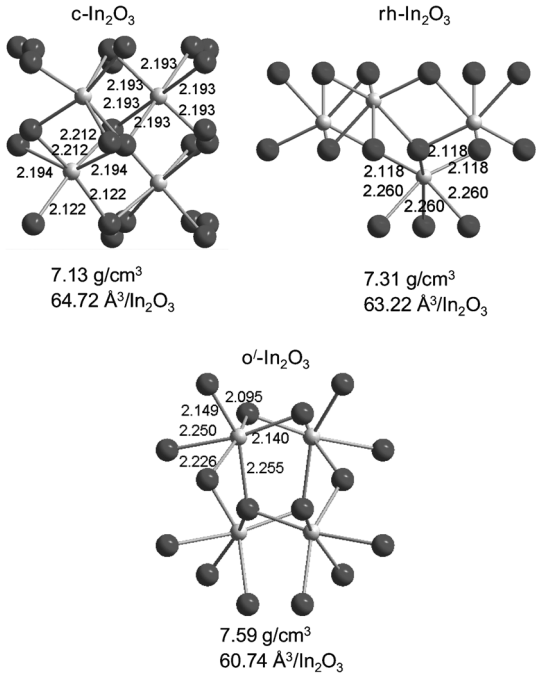

Figure 6. Coordination, density, and interatomic distances (in Å) in In_2O_3 polymorphs at ambient pressure. In and O atoms are shown as small and large balls, respectively.

provide 0.315 to 0.399 eV per formula unit of In_2O_3, as the activation barrier in this transition corresponds very well to the required energy.

In summary, we succeeded in synthesizing the orthorhombic o′-In_2O_3 polymorph from rhombohedral corundum-type rh-In_2O_3 under moderate high-pressure high-temperature conditions (8–9 GPa, 600–1100 °C) in multi-anvil and toroid apparatus. We were able to recover the polymorph to ambient pressure and temperature and to confirm its crystal structure by X-ray and electron diffraction at these conditions to be the Rh_2O_3(II)-type. Our experimental setup makes the orthorhombic o′-In_2O_3 polymorph available in large quantities for further physico-chemical characterization and provides an opportunity to grow o′-In_2O_3 as single crystals.

Received: January 14, 2013
Published online: May 6, 2013

Keywords: density-functional calculations · high-pressure reactions · oxides · phase transitions · solid-phase synthesis

[1] K. Ellmer, *Nat. Photonics* **2012**, *6*, 809–817.
[2] a) J. He, Y. F. Liu, R. Funahashi, *J. Mater. Res.* **2011**, *26*, 1762–1772; b) J. R. Sootsman, D. Y. Chung, M. G. Kanatzidis, *Angew. Chem.* **2009**, *121*, 8768–8792; *Angew. Chem. Int. Ed.* **2009**, *48*, 8616–8639.
[3] A. Gurlo, *Nanoscale* **2011**, *3*, 154–165.
[4] a) V. Scherer, C. Janowitz, A. Krapf, H. Dwelk, D. Braun, R. Manzke, *Appl. Phys. Lett.* **2012**, *100*, 212108; b) D. R. Hagleitner, M. Menhart, P. Jacobson, S. Blomberg, K. Schulte, E. Lundgren, M. Kubicek, J. Fleig, F. Kubel, C. Puls, A. Limbeck, H.

Hutter, L. A. Boatner, M. Schmid, U. Diebold, *Phys. Rev. B* **2012**, *85*, 115441; c) Z. Galazka, R. Uecker, K. Irmscher, D. Schulz, D. Klimm, M. Albrecht, M. Pietsch, S. Ganschow, A. Kwasniewski, R. Fornari, *J. Cryst. Growth* **2013**, *362*, 349 – 352.

[5] a) P. D. C. King, T. D. Veal, F. Fuchs, C. Y. Wang, D. J. Payne, A. Bourlange, H. Zhang, G. R. Bell, V. Cimalla, O. Ambacher, R. G. Egdell, F. Bechstedt, C. F. McConville, *Phys. Rev. B* **2009**, *79*, 205211; b) S. Lany, A. Zakutayev, T. O. Mason, J. F. Wager, K. R. Poeppelmeier, J. D. Perkins, J. J. Berry, D. S. Ginley, A. Zunger, *Phys. Rev. Lett.* **2012**, *108*, 016802.

[6] A. Gurlo, P. Kroll, R. Riedel, *Chem. Eur. J.* **2008**, *14*, 3306 – 3310.

[7] H. Yusa, T. Tsuchiya, J. Tsuchiya, N. Sata, Y. Ohishi, *Phys. Rev. B* **2008**, *78*, 092107.

[8] H. Yusa, T. Tsuchiya, N. Sata, Y. Ohishi, *Phys. Rev. B* **2008**, *77*, 064107.

[9] A. Gurlo, D. Dzivenko, P. Kroll, R. Riedel, *Phys. Status Solidi RRL* **2008**, *2*, 269 – 271.

[10] a) B. Xu, H. Stokes, J. J. Dong, *J. Phys. Condens. Matter* **2010**, *22*, 315403; b) A. Möller, P. Schmidt, M. Wilkening, *Nachr. Chem.* **2009**, *57*, 239 – 251; c) F. J. Manjón, D. Errandonea, *Phys. Status Solidi B* **2009**, *246*, 9 – 31.

[11] C. Wessel, R. Dronskowski, *J. Solid State Chem.* **2013**, *199*, 149 – 153.

[12] G. K. Rozenberg, L. S. Dubrovinsky, M. P. Pasternak, O. Naaman, T. Le Bihan, R. Ahuja, *Phys. Rev. B* **2002**, *65*, 064112.

[13] J. F. Lin, O. Degtyareva, C. T. Prewitt, P. Dera, N. Sata, E. Gregoryanz, H. K. Mao, R. J. Hemley, *Nat. Mater.* **2004**, *3*, 389 – 393.

[14] a) D. Liu, W. W. Lei, B. Zou, S. D. Yu, J. Hao, K. Wang, B. B. Liu, Q. L. Cui, G. T. Zou, *J. Appl. Phys.* **2008**, *104*, 083506; b) J. Qi, J. F. Liu, Y. He, W. Chen, C. Wang, *J. Appl. Phys.* **2011**, *109*, 063520.

[15] a) M. Epifani, P. Siciliano, A. Gurlo, N. Barsan, U. Weimar, *J. Am. Chem. Soc.* **2004**, *126*, 4078 – 4079; b) A. Gurlo, S. Lauterbach, G. Miehe, H.-J. Kleebe, R. Riedel, *J. Phys. Chem. C* **2008**, *112*, 9209 – 9213.

[16] T. Irifune, *Mineral. Mag.* **2002**, *66*, 769 – 790.

[17] E. Horvath-Bordon, R. Riedel, A. Zerr, P. F. McMillan, G. Auffermann, Y. Prots, W. Bronger, R. Kniep, P. Kroll, *Chem. Soc. Rev.* **2006**, *35*, 987 – 1014.

[18] M. Schwarz, T. Barsukova, C. Schimpf, D. Šimek, C. Lathe, D. Rafaja, E. Kroke in *HASYLAB Users' Meeting*, Hamburg, Germany, **2010**.

[19] M. F. Bekheet, M. Schwarz, M. Mueller, S. Lauterbach, H. J. Kleebe, R. Riedel, A. Gurlo, *RSC Adv.*, **2013**, *3*, 5357 – 5360.

[20] L. G. Khvostantsev, V. N. Slesarev, V. V. Brazhkin, *High Pressure Res.* **2004**, *24*, 371 – 383.

[21] A. N. Christensen, N. C. Broch, *Acta Chem. Scand.* **1967**, *21*, 1046 – 1056.

[22] a) D. A. Rusakov, A. A. Belik, S. Kamba, M. Savinov, D. Nuzhnyy, T. Kolodiazhnyi, K. Yamaura, E. Takayama-Muromachi, F. Borodavka, J. Kroupa, *Inorg. Chem.* **2011**, *50*, 3559 – 3566; b) A. A. Belik, T. Furubayashi, H. Yusa, E. Takayama-Muromachi, *J. Am. Chem. Soc.* **2011**, *133*, 9405 – 9412; c) C. A. Hoel, J. M. G. Amores, E. Moran, M. A. Alario-Franco, J. F. Gaillard, K. R. Poeppelmeier, *J. Am. Chem. Soc.* **2010**, *132*, 16479 – 16487.

[23] A. Walsh, C. R. A. Catlow, A. A. Sokol, S. M. Woodley, *Chem. Mater.* **2009**, *21*, 4962 – 4969.

[24] http://www.webelements.com/indium/bond_enthalpies.html.

